# IMPLEMENTATIONAND ANALYSIS OF TORQUE RIPPLE MINIMIZATION OF BLDC MOTOR USING RCHCC

**[1]D.Gopalakrishnan, [2]Dr.V. Gopalakrishnan**
[1]Assistant professor , Sri Ramakrishna Polytechnic College, Coimbatore,
[2]Associate professor, Department of Electrical and electronics engineering, GCT, Coimbatore
gkresearchmail@gmail.com, vgopalakrishnan@gct.ac.in

***Abstract*--Torque ripple minimization using simple reference controlled Hysteresis current controller is proposed in this paper. An ideal BLDC motor has trapezoidal back EMF waveform. Non-uniformity of magnetic material and design parameters are some of the practical reasons which disturb the production of exact trapezoidal wave shape. This paper introduces reference controlled Hysteresis current controller to minimize torque ripple. Performance analysis of the proposed system is analyzed using Matlab and compared with an un-ideal back EMF method. Validation of simulation analysis is proposed using the embedded system based hardware with FHP BLDC motor.**

***Keywords*-- Torque ripple minimization, BLDC, un-ideal back EMF method, reference controlled Hysteresis current controller (RCHCC), Embedded System, commutation, hysteresis bandwidth.**

## 1. INTRODUCTION

BLDC motors widely used for its advantages of simple mechanical construction, small size, light weight, easy maintenance, simple rotor cooling, good reliability and high efficiency. Brushless DC motors use the rotating permanent magnet in the rotor and stationary electrical magnets on the motor housing. The high-performance, small-diameter magnetic rotors reduce the inertia of the armature, a reduction in rotational losses, allowing high acceleration rates, and smoother servo characteristics. This optimal motor response also allows constant speeds, instant speed regulation, and a quieter drive system.

Many researchers have focused on improvement of the performance related to the current loop, speed loop, and/or position loop [1],[2]. But when VSI is utilized, the current ripple is generated by the phase current commutation. In the period of commutation current ripple is produced which results in torque ripple. The necessary di/dt in the commutation period cannot be produced by the current controller, since the motor windings are inductive, even in a finite DC bus supply voltage. Therefore, torque ripple appears such that rectangular current is fed to conventional control. Consequently, vibrations and acoustic noise in the high precision machines are caused due to speed fluctuations, resonance in mechanical portions of the drive, by the unwanted torque ripple in BLDC motor drives. As a result, the major research works are focused on commutation torque ripple, and the torque ripple reduction and upgrading the control performance of BLDC have been the research hotspot in recent years.

The BLDC motor torque ripple can be reduced either by the improving control scheme or by improving the motor design. Improved motor control scheme include adaptive control technique, pre-programmed current waveform control, selective harmonic injection technique, estimators and observers, speed loop disturbance rejection, high-speed current regulators, commutation torque minimizations and automated self-commissioning schemes. On the other hand, fractional slot winding, skewing the slots, increased number of phases, short-pitch winding, design in rotor magnet pole arc, its position, air gap windings, adjusting stator slot opening and wedges, and width characterize the improved motor designs.

G. Ranjithkumar and K.N.V Prasad [2012] [3] analyzed to build a Cascaded H-Bridge MLI with the help of current controller modulation method for BLDC motor using PSIM. P.Devendra, Ch.PavanKalyan, K.AliceMary, Ch.Saibabu [2013] [4] discussed the Optimal torque control schemes for BLDC motors reducing torque ripples using direct torque control. C.Senthil Kumar, N.Senthil Kumar, P.Radhika [2014] [5] analyzed an approach to reduce torque ripples by controlling the voltage while maintaining speed. E. Kaliappan and C. Sharmeela[2010] [6] discussed the Minimization of torque ripple in PMBLDC motor by employing L-C Filter ripple is reduced, and PID Controller is tuned using Genetic Algorithm (GA). Somesh Vinayak Tewari, B.Indu Rani [2009] [7] discussed a method of torque ripple minimization of brushless dc (BLDC) motors, with un-ideal back EMF.Recently, in order to reduce current ripple, numerous current controls have been proposed [8-10]. The typical methods are PWM current control and hysteretic current control [11]. First of all, the former has varying switching frequency, fastest speed of response, adjustable filter size, and current ripple depends on $\Delta i$. In contrast, the later has fixed switching frequency, fixed ripple current, fast speed of response, filter size is usually small and less switching loss [12, 13]. An un-ideal back EMF method for torque ripple control of BLDC motor is analyzed by Haifeng Lu in 2008 [14].

This paper presents a comprehensive analysis of the commutation torque ripple and HCC method in brushless dc motor drives. Note that the cogging torque and slot effect are not considered in this work. To enhance the current control performance, a hysteresis current controller is employed. During the commutation interval, balancing the slopes of incoming and outgoing phase currents is done by the proposed

control scheme. The triggering pulse used to operate the inverter is calculated in the hysteresis current controller during commutation period. This method operates optimal performance over the entire speed range despite being simple. To validate simulation analysis hardware is proposed using an embedded system based BLDC drive. Simulation and experimental analysis are proposed in this paper.

## 2. DYNAMIC MODEL OF THE BLDC MOTOR

In this paper, BLDC motor is fed by PWM controlled Voltage source inverter. The speed of the BLDC motor is controlled by adjusting the stator voltage of the machine. Block diagram of VSI fed BLDC motor is shown in figure 1.

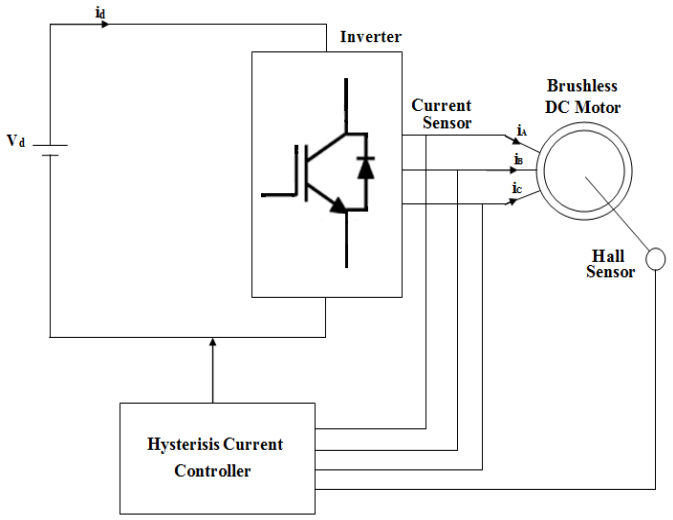


**FIG.1.** Block diagram of VSI fed BLDC motor

The model of BLDC motor [15, 16] is developed with the assumption that there is no power loss in an inverter, and then the voltage of the stator winding can be stated as,

$U_a=R_ai_a+L_a(di_a/dt)+ M_{ab}(di_b/dt)+ M_{ac}(di_c/dt)+e_a$ (1)

$U_b=R_bi_b+L_b(di_b/dt)+ M_{ba}(di_a/dt)+ M_{bc}(di_c/dt)+e_b$ (2)

$U_c=R_ci_c+L_c(di_c/dt)+ M_{ac}(di_a/dt)+ M_{bc}(di_b/dt)+e_c$ (3)

Where,

$R_a, R_b, R_c$ – Resistance of the stator winding,

$L_a, L_b, L_c$ – Self-inductance of the stator winding,

$M_{ab}, M_{ba}, M_{ac}$- Mutual inductance of the stator winding,

$e_a, e_b, e_c$- back emf of the motor,

Its equivalent circuit is shown in figure 2.

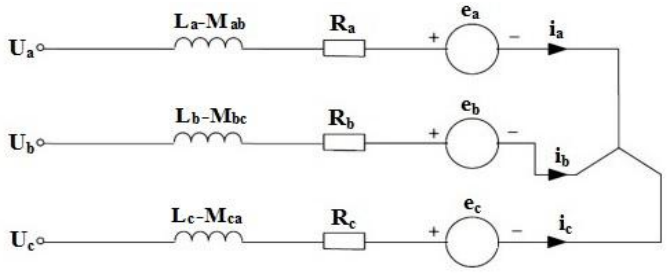


**FIG.2.** Equivalent Circuit of BLDC Motor.

Back EMF e is derived from the angular velocity of the rotor.

Where $k_e$ is back-EMF constant, $f_a(\theta)$, $f_b$ $(\theta)$ *and* $f_c(\theta)$ are functions of rotor position.

The trapezoidal shape functions of back-EMF are constant with limit values between +1, -1.

$$f_a(\theta)=\begin{cases}\left(\frac{6}{\pi}\right)\theta & 0<\theta\leq\frac{\pi}{6}\\ 1 & \frac{\pi}{6}<\theta\leq\frac{5\pi}{6}\\ -\left(\frac{6}{\pi}\right)\theta+6 & \frac{5\pi}{6}<\theta\leq\frac{7\pi}{6}\\ -1 & \frac{7\pi}{6}<\theta\leq\frac{11\pi}{6}\\ -\left(\frac{6}{\pi}\right)\theta-12 & \frac{11\pi}{6}<\theta\leq 2\pi\end{cases} \quad (4)$$

$$f_b(\theta)=\begin{bmatrix}-1 & 0<\theta\leq\frac{\pi}{6}\\ \left(\frac{6}{\pi}\right)\theta-4 & \frac{\pi}{2}<\theta\leq\frac{5\pi}{6}\\ 1 & \frac{5\pi}{6}<\theta\leq\frac{9\pi}{6}\\ -\left(\frac{6}{\pi}\right)\theta+10 & \frac{9\pi}{6}<\theta\leq\frac{11\pi}{6}\\ -1 & \frac{11\pi}{6}<\theta\leq 2\pi\end{bmatrix} \quad (5)$$

$$f_c(\theta)=\begin{bmatrix}-1 & 0<\theta\leq\frac{\pi}{2}\\ -\left(\frac{6}{\pi}\right)\theta+2 & \frac{\pi}{6}<\theta\leq\frac{\pi}{2}\\ -1 & \frac{\pi}{2}<\theta\leq\frac{7\pi}{6}\\ \left(\frac{6}{\pi}\right)\theta-8 & \frac{7\pi}{6}<\theta\leq\frac{9\pi}{6}\\ 1 & \frac{9\pi}{6}<\theta\leq 2\pi\end{bmatrix} \quad (6)$$

The functions of back EMF are as follows

$$e_a=\begin{bmatrix}\left(\frac{6E}{\pi}\right)\theta & 0<\theta\leq\frac{\pi}{6}\\ E & \frac{\pi}{6}<\theta\leq\frac{5\pi}{6}\\ -\left(\frac{6E}{\pi}\right)\theta+6E & \frac{5\pi}{6}<\theta\leq\frac{7\pi}{6}\\ -E & \frac{7\pi}{6}<\theta\leq\frac{11\pi}{6}\\ -\left(\frac{6E}{\pi}\right)\theta-12E & \frac{11\pi}{6}<\theta\leq 2\pi\end{bmatrix} \quad (7)$$

$$e_b=\begin{bmatrix}-E & 0<\theta\leq\frac{\pi}{6}\\ \left(\frac{6E}{\pi}\right)\theta-4E & \frac{\pi}{2}<\theta\leq\frac{5\pi}{6}\\ E & \frac{5\pi}{6}<\theta\leq\frac{9\pi}{6}\\ -\left(\frac{6E}{\pi}\right)\theta+10E & \frac{9\pi}{6}<\theta\leq\frac{11\pi}{6}\\ -E & \frac{11\pi}{6}<\theta\leq 2\pi\end{bmatrix} \quad (8)$$

$$e_c = \begin{bmatrix} -E & 0 < \theta \leq \frac{\pi}{2} \\ -\left(\frac{6E}{\pi}\right)\theta + 2E & \frac{\pi}{6} < \theta \leq \frac{\pi}{2} \\ -E & \frac{\pi}{2} < \theta \leq \frac{7\pi}{6} \\ \left(\frac{6E}{\pi}\right)\theta - 8E & \frac{7\pi}{6} < \theta \leq \frac{9\pi}{6} \\ E & \frac{9\pi}{6} < \theta \leq 2\pi \end{bmatrix} \quad (9)$$

By comparing (4-6) with (7-9) back EMF can be expressed as follows

$$\begin{bmatrix} e_a \\ e_b \\ e_c \end{bmatrix} = E \begin{bmatrix} f_{a\,(\Theta)} \\ f_b(\Theta) \\ f_c(\Theta) \end{bmatrix} \quad (10)$$

$$E = k_e \omega_r \quad (11)$$

The torque of the BLDC motor is derived from the back emf, stator current, and speed.

$$T_{em} = (e_a . i_a + e_b . i_a + e_c . i_a)/w_m \quad (12)$$

From speed and Torque characteristics of BLDC motor

$$\omega_m = \frac{P}{2J} \int [(T_a + T_b + T_c) - T_L] d \quad (13)$$

$$T_e - T_L = J \frac{d\omega_m}{dt} + B\omega_m \quad (14)$$

From the above equations model of BLDC motor can be developed.

The balanced stator phase currents are considered to be as in (15)

$$i_a + i_b + i_c = 0 \quad (15)$$

In the commutation period, it is gained as follows

$$e_a = e_b = e_c = E_m \quad (16)$$

Then the torque during the commutation can be written

$$T_e = \frac{2E_m}{\omega}\left(I_0 + \frac{V_d - 4E_m}{3L} t\right) \quad (17)$$

Consider a case of commutation without the effect of HCC and consider that the circuit status changes from phase A and phase C's turn-on to phase B and phase C's turn-on, phase A current flows D4 and decays to zero slowly, while phase B current progressively increases to the maximum and reaches its steady-state value. In the period of commutation, circuit equation can be given as follows.

$$L \frac{di_a}{dt} + r i_a + e_a - \left(L \frac{di_c}{dt} + r i_c + e_c\right) = 0 \quad (18)$$

$$L \frac{di_b}{dt} + r i_b + e_b - \left(L \frac{di_c}{dt} + r i_c + e_c\right) = V_d$$

The |ri_x | is very lesser than|L (di_x)/(di_t )| (x= a,b,c) when compared with the winding time constant L/R of a BLDC motor. Consequently, the effect of the armature winding resistance can be neglected. Furthermore the initial and ultimate values of every phase current equal every phase steady-state current value I0 before and after the commutation. All phase currents during the commutation can be obtained from (15) to (18)

$$i_a = I_0 - \frac{V_d + 2E_m}{3L} t$$

$$i_b = \frac{2(V_d - E_m)}{3L} t \quad (19)$$

$$i_c = -I_0 - \frac{V_d - 4E_m}{3L} t$$

From (19), the turn-off time $t_{-off}$ of phase A and the turn-on time $t_{-on}$ of phase B during the commutation process are

$$t_{-off} = \frac{3LI_0}{V_d + 2E_m} \quad (20)$$

$$t_{-on} = \frac{3LI_0}{2(V_d - E_m)} \quad (21)$$

From (17),(19-21), the commutation between two phases can't be completed in the same time as $U_d > 4E_m$, i.e., the motor speed is less than a certain value, and as a result $i_B$ has reached its steady-state value before $i_A$ falls to 0, shown in figure 3.(I). Furthermore, the commutation guides to a raise in the amplitude of torque. The ripple in torque can be attained

$$T_r = \frac{E_m I_0}{\omega} * \frac{V_d - 4E_m}{U_d - E_m} \quad (22)$$

Between two phases the commutation can be finished in the same time as $U_d = 4E_m$, i.e., the motor runs at definite speed, and as a result, $i_B$ has exactly reached its steady-state value when $i_A$ falls to 0, shown in figure 3.(II). In this case, during the commutation, the torque remains constant, and its value equals the torque in the period of the non-commutation process.

$$T_e = \frac{2E_m I_0}{\omega} \quad (23)$$

As $V_d < 4E_m$, i.e., the motor speed is larger than a definite value, the commutation among two phases can't finished in the same time, and as consequence $i_B$ doesn't attain its steady-state value when $i_A$ falls to 0, shown in figure 4. (III). The commutation leads to a decrease in the amplitude of torque. The torque ripple can be obtained

$$T_r = \frac{2E_m I_0}{\omega} * \frac{V_d - 4E_m}{V_d + 2E_m} \quad (24)$$

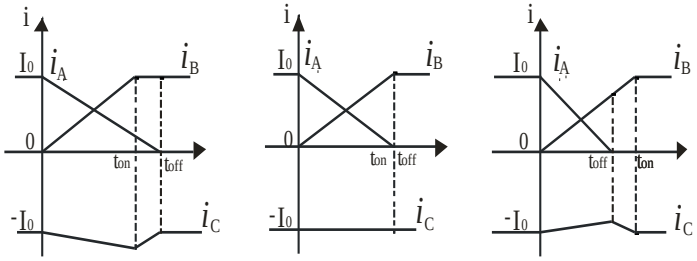


**FIG.3.** Phase Currents during Commutation In various Cases

## 3. OPERATION OF HYSTERESIS CURRENT CONTROLLER

In various medium and low voltage utility applications Hysteresis Current controlled inverter is utilized. Mainly depends on the particular switching pattern functional to the valves, the line harmonic is generated from the inverter. The block diagram of hysteresis current controller is shown in Fig.4 which will produce the gating pulses for the inverter. The reference currents, $i_a$*, $i_b$*, $i_c$* are compared with measured actual input currents, $i_a$, $i_b$, $i_c$. The comparator receives an error with a specified hysteresis band. Switching of the power semiconductor devices (S1 ON and S2 OFF) occurs when the current attempts to surpass a put value equivalent to the desired current. The reverse switching (S1 OFF and S2 ON) occurs when the current attempts to turn into fewer than $i_a$*. If the real current is extra than the given value, then it is abridged by altering the switching state and vice versa. The actual current varies around the reference current waveform and hysteresis current control makes the variation within a convinced range [17].

Hysteresis controller is easy to implement and produces an extremely good quality of waveform. The downside of this method is that the switching frequency does not linger invariable but varies along dissimilar portions of the desired current. The switching pattern is given as:

If $\Delta i_a$>H, S1 is on and S2 is off.

If $\Delta i_a$<L, S1 is off and S2 is on.

If $\Delta i_b$>H, S3 is on and S4 is off.

If $\Delta i_b$<L, S3 is off and S4 is on.

If $\Delta i_c$>H, S5 is on and S6 is off.

If $\Delta i_c$<L, S5 is off and S6 is on.

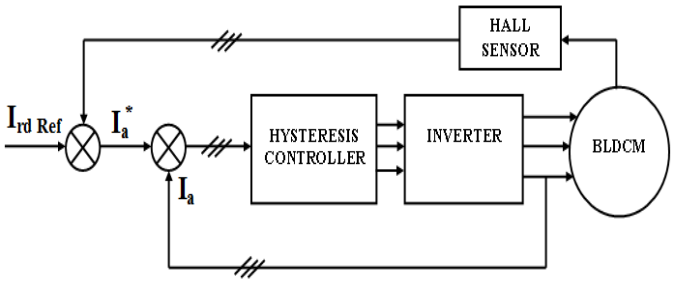


**FIG.4.** Block diagram of HCC

Where $\Delta i_a = i_a^* - i_a$ and L, H are the lower and higher limits of hysteresis band. Consequently, by controlling the current required quasi-square waveforms can be attained.

The switching frequency of the hysteresis band current control method described above depends on how fast the current changes from the upper limit of the hysteresis band to lower limit of the hysteresis band, or vice versa. The rate of change of the actual line current vary the switching frequency; consequently, the switching frequency does not constantly linger the whole time of the switching function, however, changes along with the current waveform. Furthermore, the line inductance value of the motor and the dc link voltage are the main parameters determining the rate of change of line currents. The switching frequency of the system also depends on the voltage and the line inductances of the motor.

The bandwidth of the hysteresis current controller determines the permissible current shaping error. By varying the bandwidth the user can control the normal switching frequency and evaluate the performance for different values of hysteresis bandwidth. Though, there are device margins and escalating the switching frequency causes increased switching losses and EMI allied problems. The assortment of switching frequencies used is based on a compromise flanked by these factors. The hysteresis band current control scheme is commonly used since its straightforwardness of execution, among the different PWM techniques. Further quick-response current loop and inherent-peak current limiting ability, the method does not require any data about system parameters. Yet, the current control with a preset hysteresis band has the drawback that the switching frequency varies within a band as peak to peak current ripple is required to be controlled at all points of the essential frequency wave.

### 3.1. Hysteresis bandwidth calculation

Figure 5 shows the HCC wave for phase A.

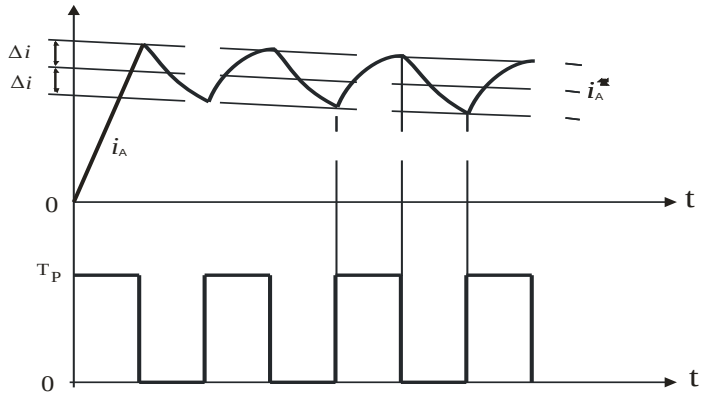


**FIG.5.** Hysteresis Controller Output Waveform

At point 1 the $i_A$ currents tend to cross the lower hysteresis band, where the switch $S_1$ is switched on. The linearly rising current ($i_A$) then touches the upper band at point 2, where the switch $S_1$ is switched off. The following equation can be written in the respective switching intervals $t_1$ and $t_2$ from Figure 5.

$$\frac{di_A^+}{dt} = \frac{1}{L}(0.5V_{dc} - E_m) \quad (25)$$

$$\frac{di_A^-}{dt} = -\frac{1}{L}(0.5V_{dc} + E_m) \quad (26)$$

From the geometry of Figure 5 can be written,

$$\frac{di_A^+}{dt}t_1 - \frac{di_A^*}{dt}t_1 = 2\text{HB} \quad (27)$$

$$\frac{di_A^-}{dt}t_2 - \frac{di_A^*}{dt}t_2 = -2\text{HB} \quad (28)$$

$$t_1 + t_2 = T_c = \frac{1}{f_c} \quad (29)$$

Where $t_1$and $t_2$ are the respective switching intervals, and $f_c$ is the switching frequency.

Adding (27) and (28) and substituting (29), it can be written

$$t_1 \frac{di_A^+}{dt} + t_2 \frac{di_A^-}{dt} - \frac{1}{f_c}\frac{di_A^*}{dt} = 0 \qquad (30)$$

Subtracting (28) from (27), we get

$$4\text{HB} = t_1 \frac{di_A^+}{dt} - t_2 \frac{di_A^-}{dt} - (t_1 + t_2)\frac{di_A^*}{dt} \qquad (31)$$

Substituting (28) in (31), gives

$$4\text{HB} = (t_1 + t_2)\frac{di_A^+}{dt} - (t_1 - t_2)\frac{di_A^*}{dt} \qquad (32)$$

Substituting (30) in (32), simplifying

$$t_1 - t_2 = \frac{di_A^*/dt}{f_c(di_A^+/dt)} \qquad (33)$$

Substituting (32) in (26), gives

$$\text{HB} = \left\{\frac{0.125V_{dc}}{f_c L}\left[1 - \frac{4L^2}{V_{dc}^2}\left(\frac{E_m}{L} + m\right)^2\right]\right\} \qquad (34)$$

Where $f_c$ is modulation frequency, $m = di_A^*/dt$ is the slope of command current wave. Hysteresis band (HB) can be modulated at diverse points of basic frequency cycle to control the switching pattern of the inverter. For the symmetrical operation of all three phases, it is expected that the hysteresis bandwidth profiles $HB_A$, $HB_B$ and $HB_C$ will be same, except have phase disparity. The adaptive hysteresis band current controller changes the hysteresis band current controller changes the hysteresis bandwidth according to instantaneous compensation current variation $di_A^*/dt$ and $V_{dc}$ voltage to minimize the influence of current distortion on the modulated waveform.

Eq.(21) shows the hysteresis bandwidth(HB) as a function of modulation frequency, supply voltage, line inductance and slope of the ic* reference compensator current wave. Hysteresis band can be modulated as a function of $V_{dc}$ and $m$ so that the modulation frequency $f_c$ remains constant. This will improve the PWM performance.

## 4. TORQUE CONTROL USING UN-IDEAL BACK EMF METHOD

In the Un-ideal Back EMF (UIBEMF) method the slope of outgoing phase current is slowed down when the estimated duty ratio reaches its 100% but still the torque feedback not able to follow the reference torque. The slowed down can be attained by turn on the upper switch of phase to compensate the current dip in the uncompensated previous phase current and also commutation torque ripple.

In the period of commutation, three phase voltage equations can be written as

$$\begin{cases} \dfrac{V_{dc}}{2} = Ri_a + L\dfrac{di_a}{dt} + e_a + V_{no} \\ -\dfrac{V_{dc}}{2} = Ri_b + L\dfrac{di_b}{dt} + e_b + V_{no} \\ S.\dfrac{V_{dc}}{2} = Ri_c + L\dfrac{di_c}{dt} + e_c + V_{no} \end{cases} \qquad (35)$$

The current slope of phase A With the switching function S can be expressed as

$$\frac{\mathrm{di_a}}{\mathrm{dt}} = \begin{cases} \dfrac{\mathrm{V_{dc}}}{3\mathrm{L}} + \dfrac{\mathrm{e_b} + \mathrm{e_c} - 2\mathrm{e_a}}{3\mathrm{L}}, & \text{at } \mathrm{S} = 1 \\ \dfrac{2\mathrm{V_{dc}}}{3\mathrm{L}} + \dfrac{\mathrm{e_b} + \mathrm{e_c} - 2\mathrm{e_a}}{3\mathrm{L}}, & \text{at } \mathrm{S} = -1 \end{cases} \qquad (36)$$

Solving (36) results in current of phase a as follows

$$\mathrm{i_{a(k+1)}} = \frac{\mathrm{T_S}}{3\mathrm{L}}\left[\mathrm{U_{dc(k)}}\left(3\mathrm{D_{c(k)}} - 1\right) + \mathrm{e_{b(k)}} + \mathrm{e_{c(k)}} - 2\mathrm{e_{a(k)}}\right] + \mathrm{i_{a(k)}} \qquad (37)$$

For an analysis consider the $i_c$ current to be slowed down, then switch S5 to be turned on with the duty ratio of $D_O$. The $D_{O\,(k)}$ for S5 is as follows

$$\mathrm{D_{o(k)}} = \frac{3\left[\mathrm{T_{ref}} - \mathrm{T_{e(k)}}\right]\omega_{\mathrm{m(k)}}\mathrm{L}}{\mathrm{V_{dc(k)}}\left[2\mathrm{e_{c(k)}} - \mathrm{e_{a(k)}} - \mathrm{e_{c(k)}}\right]\mathrm{T_s}} - \frac{2\mathrm{e_{a(k)}} - \mathrm{e_{b(k)}} - \mathrm{e_{c(k)}}}{2\mathrm{e_{c(k)}} - \mathrm{e_{b(k)}} - \mathrm{e_{a(k)}}} - \frac{\mathrm{g}\left(\mathrm{e_{a(k)}}, \mathrm{e_{b(k)}}, \mathrm{e_{c(k)}}\right)}{\mathrm{V_{dc(k)}}\left[2\mathrm{e_{c(k)}} - \mathrm{e_{a(k)}} - \mathrm{e_{b(k)}}\right]} \qquad (38)$$

Where $T_{ref}$ is the reference torque, $T_e$ is the estimated torque, $\omega_m$ is the motor speed, $V_{dc}$ is the DC voltage, $e_{a(k)}$, $e_{b(k)}$ and $e_{c(k)}$ are the three phase back emf. The duty cycle $D_O$ is used to slow down the slope of the outgoing phase current $i_c$; so as to reduce the current dip existed in the un-commutated phase $i_b$ in the commutation period, and to compensate the commutation torque ripple caused by finite dc supply voltage. When the outgoing phase current is reduced to zero, the regulation of can be stopped.

## 5. PROPOSED RCHCC TORQUE CONTROL METHOD

Even though un-ideal back EMF method has the capability of reducing torque ripple, it requires measurement of inductance, DC voltage, back EMF. Since it needs inductance to decide duty ratio, it becomes parameter dependent. The PWM or Duty ratio control of UIBEMF method is frequency controlled, so the switch is delayed by D in case of high frequency. So in this paper novel reference controlled Hysteresis Current Controller is proposed for torque ripple control in BLDC drive. The method of minimization of torque ripple using the RCHCC is described in this paper. In a proposed system rising current is sensed to delay falling current instead of sensing falling current compare to UIBEMF control.

For an analysis of the proposed scheme, the instantaneous currents are measured with the help of current sensors. The maximum torque is produced by every $60^0$ commutations in switching circuits. Because of the inductance of the armature, all the three phases are conducted concurrently. Let's presume the switchover of current from phase A to B for a solitary commutation process. This switching is performed by turning off $S_1$ and turning on $S_3$. The phase current $i_B$ increases through turn-on of $S_3$ is called an incoming current. The phase current $i_A$ decreases through turn-off of $S_1$ is called an outgoing current. The outgoing current slowly decreases through the freewheeling diode $D_1$. The current $i_c$ remains unchanged during commutation called as un-commutated phase current.

By inverting the incoming phase current the reference current is calculated by the hysteresis current controller. Reference current for each phase is calculated as follows

$$I_a^* = -I_b + I_{max} \quad (39)$$

$$I_b^* = -I_c + I_{max} \quad (40)$$

$$I_c^* = -I_a + I_{max} \quad (41)$$

Where $I_a^*$, $I_b^*$ and $I_c^*$ are reference currents produce by RCHCC. $I_{max}$ is the maximum value of current in the three phase. The width of hysteresis Band is set below and above the reference current. The Minimum and Maximum value of the instantaneous outgoing current is inside the bandwidth. The quickest current control is achievable if the bandwidth is tiny. The switches receive control pulses from HCC to enlarge the commutation period equal to the incoming current achieves 80% of its instantaneous maximum value and then simply the turn-off. The switching status of each switch in RCHCC is stated as follows

If $I_a < I_a^*$, S1 is on and S2 is off.

If $I_a > I_a^*$, S1 is off and S2 is on.

If $I_b < I_b^*$, S3 is on and S4 is off.

If $I_b > I_b^*$, S3 is off and S4 is on.

If $I_c < I_c^*$, S5 is on and S6 is off.

If $I_c > I_c^*$, S5 is off and S6 is on.

Hence the RCHCC method does not require any parameters such as inductance it is parameter independent method. The elimination of torque calculation simplifies the procedure. From the reference current calculation (39)-(41) and switching calculation it is noted that only current is considered for switching. Therefore RCHCC is simplified and parameter independent

## 6. SIMULATION RESULTS

The simulation analysis of permanent magnet brushless DC motor is done for 3 sec under various conditions-conventional control method with hysteresis control while commutation period. The phase current using conventional control method is shown in figure 6. In the period of commutation, spicks exist in un-commutated phase current. Because of this torque ripple is existed. The torque with ripple using conventional control method is shown in figure 7. The phase current and torque produced by UIBEMF method are shown in figures 8 and 9. Compare to conventional HCC current ripple is reduced by this method which shows its impact in torque control. The torque ripple is also minimized. The phase current in RCHCC control method is shown in figure 10. Current spikes are minimized during commutation period by using RCHCC. Because of this torque ripple is apparently reduced compared with traditional control. The torque produced by proposed RCHCC is shown in figure 11. Comparison performance of all methods such as conventional HCC, UIBEMF and RCHCC methods are shown in figure 12 and 13. Figure 14 Shows the Simulink model of proposed controller.

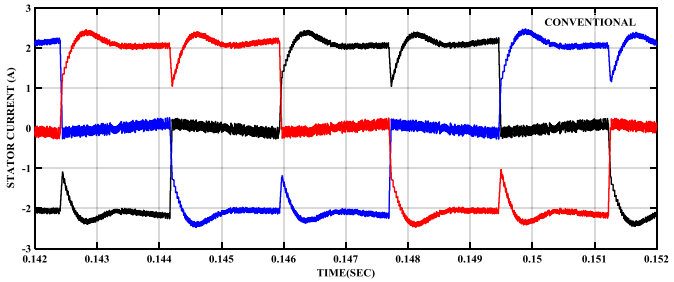


**FIG.6.** Phase current using conventional control method

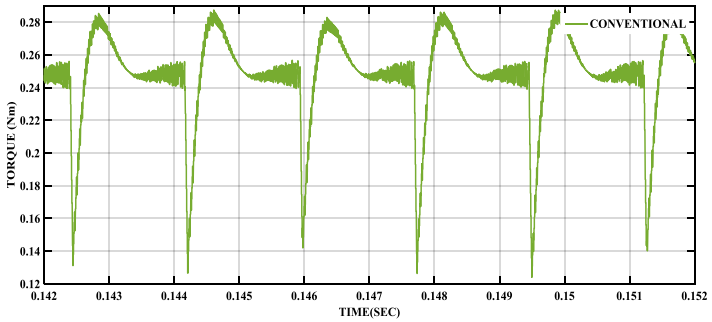


**FIG.7.** Torque with ripple using conventional control method

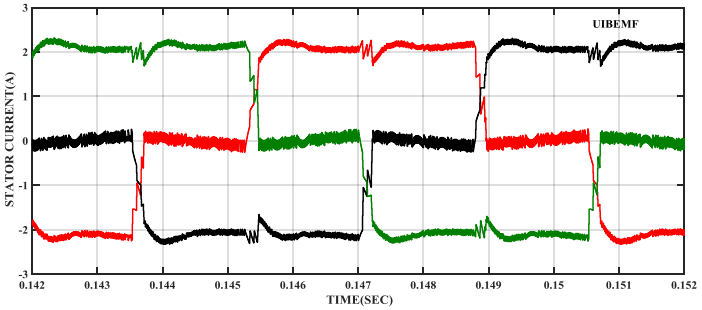


**FIG.8.** Phase current using UIBEMF method

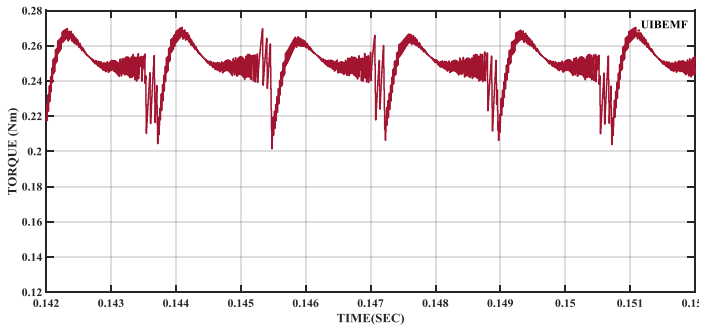


**FIG.9.** Torque with ripple using UIBEMF method

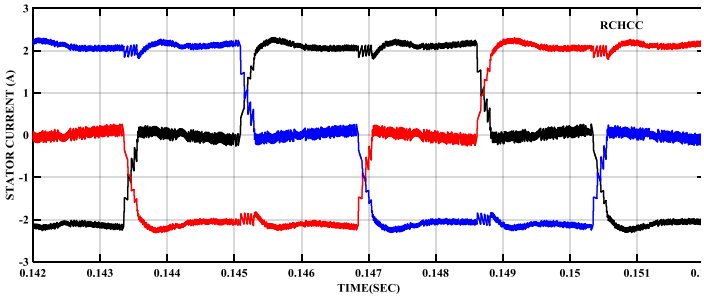


**FIG.10.** Phase current in RCHCC method

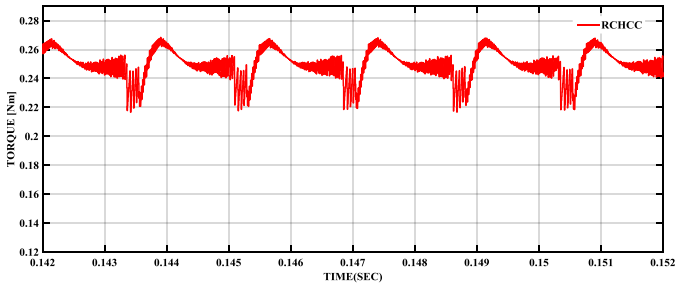


**FIG.11.** Torque produced by proposed RCHCC

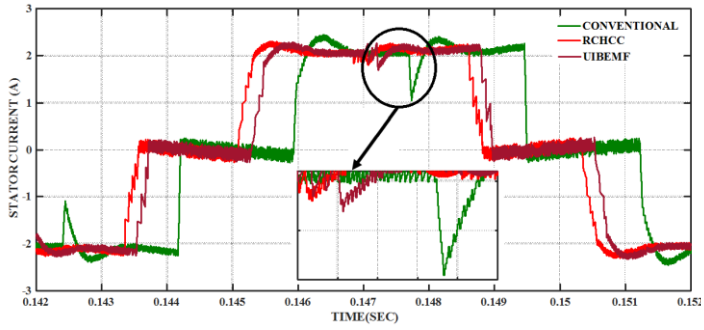


**FIG.12.** Combined R-Phase current

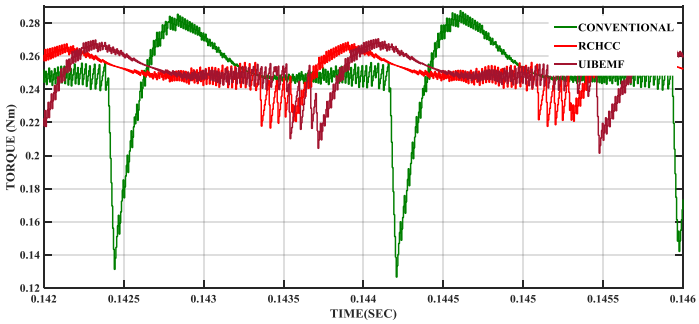


**FIG.13.** Combined Torque with ripple

From the figure 12, it is noted that compare to all other methods RCHCC reduces current ripple effectively. It results in effective torque ripple control as shown in figure 13. Table 2 shows performance comparison various controllers in BLDC motor control from the figures 12 and 13.

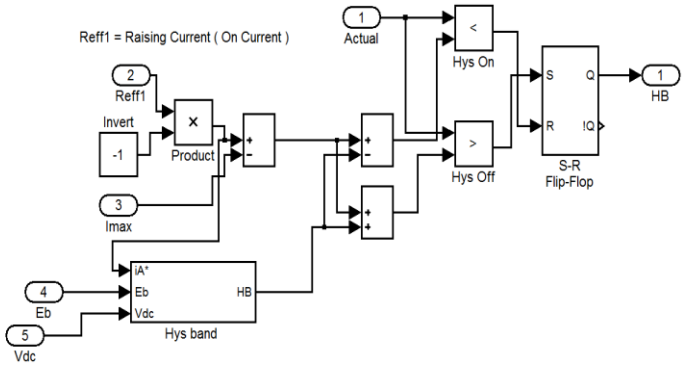


**FIG.14.** Simulink Model of proposed RCHCC

## 6.1.Motor Parameters

**TABLE1** Motor parameters

| | |
|---|---|
| Voltage | 24V |
| Power | 200W |
| Phase Resistance | 0.19 Ohm |
| Phase Inductance | 0.517 mH |
| Torque constant | 0.11 Nm/A |
| Back EMF constant | 7.0V/Krpm |

**TABLE 2** Performance of proposed hysterias controller

| Parameter | Existing HCC | UIBEMF control | Proposed RCHCC |
|---|---|---|---|
| Current ripple (A) | 0.14 | 0.032 | 0.02 |
| Torque ripple (Nm) | 0.0760 | 0.0300 | 0.0225 |

From the table 2, it is noted that the current ripple is greatly reduced by the proposed system. 77% of current ripple is reduced by UIBEMF control whereas 85% current ripple is reduced by the proposed system compared to the conventional HCC.

## 7. EXPERIMENTAL RESULTS

The effectiveness of the proposed controller performance is analyzed using experiments to confirm the simulation result. A BLDC of rating 200w, 3 phase, 24v, 3000 RPM is experimenting using the PIC16F887. It is a 40 Pin, Enhanced serial (SPI) and parallel flash memories, and efficiently integrating the functions of many chips into a PIC microcontroller. Novel torque control algorithm is programmed in the PIC. It is to build the PWM module produces triggering pulses for the inverter as per decoder program. The hex bridge inverter is designed with MOSFETs. The speed of the machine is sensed using an inductive proximity sensor. Experimental setup of the drive is shown in figure 15.

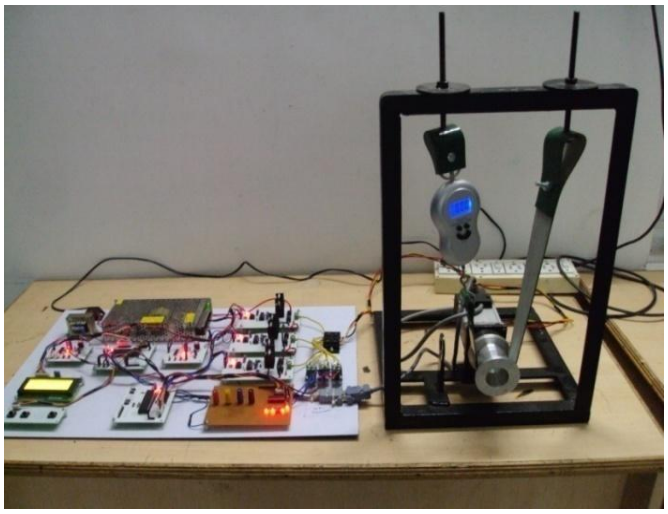

**FIG.15.** Experimental setup of the drive

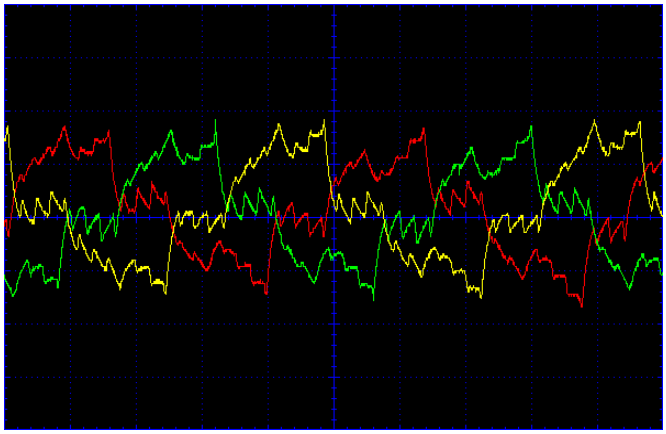

**FIG.16.** RCHCC controlled Current wave

From the figure 16, it is noted that ripple or drop in one phase current during the rising of other phase is reduced effectively with the help RCHCC in BLDC motor drive. From the simulation analysis, it is noted control in a current result in torque ripple control. Therefore from the hardware result of ripple control in current results in torque ripple control.

## 8. CONCLUSION

In this paper, reference controlled Hysteresis current controller based torque ripple minimization of BLDC motor is analyzed using Matlab. RCHCC controlled VSI supports motor to produce trapezoidal wave shape which reduces the torque ripple. It is also simple avoiding complexity in measuring various parameters of the motor like UIBEMF method. UIBEMF control reduces 77% current ripple compare to convention HCC, but it complicated and parameter dependent method. Simple control of proposed RCHCC reduces around 85% of current ripple compare to conventional HCC. Simulation analysis is validated with the experimental analysis using PIC microcontroller based 200W motor. Ripple control in the current of experimental setup validates the effectiveness of torque ripple control of proposed RCHCC method.

## REFERENCES


[1] Milivojevic, N., Krishnamurthy, M., Gurkaynak, Y., Sathyan, A., Lee, Y.J. and Emadi, A., 2012. "Stability analysis of FPGA-based control of brushless DC motors and generators using digital PWM technique", *IEEE Transactions on Industrial Electronics*, 59(1), pp.343-351. http://dx.doi.org/10.1109/TIE.2011.2146220

[2] Rodriguez. F and A. Emadi., 2007. "A novel digital control technique for brushless DC motor drives", *IEEE Transactions on Industrial Electronics*. vol. 54, no. 5, pp. 2365–2373. http://dx.doi.org/10.1109/TIE.2007.900312

[3] Ranjithkumar, G. and Prasad, K.N.V., 2012. "Minimization of torque ripple content for BLDC motor by current controller using MLI". *Procedia Engineering*, 38, pp.3113-3121. https://doi.org/10.1016/j.proeng.2012.06.362

[4] Devendra, P., Kalyan, C.P., Mary, K.A. and Saibabu, C. 2003. "Simulation approach for torque ripple minimization of BLDC motor using direct torque control". *Simulation*, Vol 2 No.8.

[5] Kumar, C.S., Kumar, N.S. and Radhika, P., 2014. "Torque ripple minimization in bldc motor using dc-dc sepic converter". *Przegląd Elektrotechniczny*, Vol 90 no.9, pp.146-150.

[6] Kaliappan, E. and Sharmeela, C. "Torque ripple minimization of permanent magnet brushless DC motor using genetic algorithm". *In Power Electronics and Instrumentation Engineering Springer Berlin Heidelberg*. Pp. 53-55. https://doi.org/10.1007/978-3-642-15739-49

[7] Tewari, S.V. and Rani, B.I. 2009. "Torque ripple minimization of BLDC motor with un-ideal back EMF". *In: Emerging Trends in Engineering and Technology (ICETET)*, 2nd International Conference on IEEE. pp. 687-690. https://doi.org/10.1109/ICETET.2009.226

[8] Ghosh, A., Santra, S.B., Maharana, M.K. and Biswal, P. 2016. "Torque ripple and efficiency optimization of a novel boost converter fed BLDC Motor Drive". *In Computation of Power, Energy Information and Commuincation, (ICCPEIC)*, International Conference on IEEE. pp. 344-349. https://doi.org/10.1109/ICCPEIC.2016.7557255

[9] Kim, D.K., Lee, K.W. and Kwon, B.I., 2016. "Commutation torque ripple reduction in a position sensorless brushless DC motor drive". *IEEE Transactions on Power Electronics*, Vol 21 No.6, pp.1762-1768. https://doi.org/10.1109/TPEL.2006.882918

[10] Park, S.H., Kim, T.S., Ahn, S.C. and Hyun, D.S., 2003. "A simple current control algorithm for torque ripple reduction of brushless DC motor using four-switch three-phase inverter". *Power Electronics Specialist Conference. PESC'03.* 34th

Annual IEEE Vol.2, pp. 574-579. https://doi.org/10.1109/PESC.2003.1218119

[11] J. W. Dixon and L. A. Leal. 2002. "Current control strategy for brushless DC motors based on a common DC signal", *IEEE Trans. On Power Electronics*, Vol. 17, Pp.232-240 https://doi.org/10.1109/63.988834

[12] A. Chauhan, R. P. Singh., 2016. "Pulse Width Modulation Based Adaptive Hysteresis Current Controller Using Intelligent Technique", *International Journal of Advanced Research in Electrical, Electronics and Instrumentation Engineering*, 2016.pp. 303-310.

[13] Punithavathani, D. Shalini, K. Sujatha, and J. Mark Jain. "Surveillance of anomaly and misuse in critical networks to counter insider threats using computational intelligence." *Cluster Computing* 18.1 (2015): 435-451.

[14] Putri, A.I., Rizqiawan, A., Rozzi, F., Zakkia, N., Haroen, Y. and Dahono, P.A. 2016. "A hysteresis current controller for grid-connected inverter with reduced losses". *In: Industrial, Mechanical, Electrical, and Chemical Engineering (ICIMECE)*, International Conference of IEEE, pp. 167-170. https://doi.org/10.1109/ICIMECE.2016.7910446

[15] Aydogdu, Omer, and Ramazan Akkaya. 2012. "Design of a Real Coded GA Based Fuzzy Controller for Speed Control of a Brushless DC Motor". *INTECH Open Access Publisher*, http://dx.doi.org/10.5772/49972

[16] Ashish A, Zanjade 2013. "Hardware Implementation of Fuzzy Logic Controller for Sensor less Permanent Magnet BLDC Motor Drives". *International Journal of Engineering Research & Technology*; vol 2:4.

[17] Y. L. Wang, Q. L. Guo, 2011. "Hysteresis Current Control technique based on Space Vector Modulation for Active Power Filter", *International Journal of Power Electronics and Drive System*, vol.1, no.1, pp. 1-6. https://doi.org/10.4028/www.scientific.net/AMM.385-386.1224

**Author – 1 (D.Gopalakrishnan)**

D.Gopalakrishnan qualified B.E in EEE from Coimbatore Institute of technology, Coimbatore in 2003, and received his M.E Degree from Sri Ramakrishna Engineering College, Coimbatore in the field of "Power Electronics &Derives". Currently pursuing his Ph.D in Brushless DC motor Drives from Anna University, Chennai. After B.E, he worked in Turbo systems, Coimbatore as a Design & Development Engineer for three years. Since 2006 he is teaching at Sri Ramakrishna Polytechnic College, Coimbatore and interested to be involved in research on DC Drives. He had published several reputed papers in International Journals and attended National and International Conferences.

---

**Author – 2 (Dr.V.Gopalakrishnan)**

Dr. V. Gopalakrishnan received the Ph.D. degree in Information and Communication Engineering from Anna University, Chennai, Tamil Nadu, India, Received the M.E. degree in Computer Science and Engineering from Government College of Technology, Coimbatore, India; He presented more than 20 papers in National and International Conferences and also he published more than 10 papers in National and International Journals. His research interests include power system protection, high voltage engineering, computer network, wireless sensor networks, renewable energy resources.

---